Article can be accessed online at http://www.publishingindia.com

Novel Algorithm for Image Segmentation Using Neural Network

Sadegh Nezarat[*], Ali Ghareaghaji[**], Hamed Bazyar[***], Seyed Arsalan Hossini [****]

Abstract

The pulse-coupled neural network (PCNN) is widely used in image segmentation. However, the determination of parameter values in the PCNN framework is an unavoidable and trivial task that may cause neurons to behave unexpectedly, thus affecting segmentation performance. Therefore, this paper presents an efficient iterative algorithm using a modified PCNN for automatic image segmentation. In contrast to existing PCNN models, a new neural threshold was first established for the modified PCNN instead of a general dynamic threshold, allowing for greater efficiency in controlling the pulse output.

Besides, a varying linking coefficient value was constructed for efficiently adjusting the neural behavior. By incorporating the Bayes clustering method, it thereby extends the feasibility of the model for the extraction of targets with inhomogeneous brightness, thus resulting in a simpler iterative algorithm for segmentation. Experiments on real-world infrared images demonstrate the efficiency of our proposed model. Moreover, compared with simplified PCNN models and classic segmentation methods, the proposed model shows fewer misclassification errors and higher segmentation performance.

Keywords: Pulse-Coupled, Neural, Network, Image Segmentation, Neural Threshold, Bayes Clustering Method.

1. Introduction

The pulse-coupled neural network (PCNN) simulates the synchronous oscillation phenomenon in the visual cortex of cats [1], and offers great potential for image processing. Up to now, the PCNN model has been widely used in image segmentation [2–8]. In contrast to other segmentation algorithms, two significant mechanisms are inherent in the PCNN: (1) synchronous oscillation causes the fired neuron to capture neurons based on spatial proximity and brightness similarity; (2) the dynamic threshold mechanism enables the model to generate temporal series of pulse outputs through iterative computation for obtaining a pulse output as the final result. However, the performance of the final result significantly depends on the determination of PCNN parameter values.

The PCNN has numerous parameters that are not easily applied into real-world image segmentation [9]. Thus, researchers focused on the simplified PCNN (SPCNN) [10–12] and attended to automatically deal with SPCNN parameters for binary segmentation purpose. Kuntimad and Ranganath [10] analyzed the range values of linking coefficients to achieve perfect image segmentation when the intensity ranges of adjacent regions overlap. Ma [13] introduced the maximum entropy principle for segmented images to stop the iteration after manually setting the parameters. Later, Ma [14] established an automated SPCNN system based on genetic algorithm to estimate the proper values of parameters through heavy training.

* Electronic Engineering Department, Bushehr Branch Islamic Azad University, Bushehr, Iran.
E-mail: senzarat@yahoo.com
** Electrical and Computer Engineering Department, Shahid Beheshti University,Tehran, Iran.
E-mail: a.ghareaghaji@mail.sbu.ac.ir
*** Electronic Engineering Department,Bushehr Branch Islamic Azad University,Bushehr, Iran.
E-mail: hamedbazyar30@yahoo.com
**** Electronic Engineering Department, Bushehr Branch Islamic Azad University, Bushehr, Iran.
E-mail: arsalanho@yahoo.com

Bi [15] proposed a method that adaptively deter mines the weight matrixes and linking coefficients by using spatial and gray characteristics, but requires the repetition of trails to adjust the constant of the dynamic threshold. Wei [2] focused on the threshold time constant of the SPCNN through the overall characteristics of the image and manually allocated other parameters. Chen [12] determined all adjustable parameters by analyzing the relationship between the static properties of input images and the dynamic properties of neurons. Nevertheless, the determination of these adjustable parameters does not completely depend on the static properties of input images and the dynamic properties of neurons. Raya [16] presented a quantitative approach for the automatic and direct computation of the linking coefficient and primary firing threshold directly from the image histogram. Deng [17] analyzed the firing mechanism of neurons and modified the formulas of the firing time for automatic image segmentation.

However, determining the appropriate values for the linking coefficient and dynamic threshold still remains a challenge and necessitates further research. In the current paper, we employed the PCNN framework to develop a novel iterative algorithm for image segmentation. We present an effective neural threshold that can be updated by the cluster centers through PCNN iteration.

Since the pulse output is strongly affected by the linking coefficient value, a varying linking coefficient was constructed to encourage neurons with spatial proximity to pulse together. The Bayes clustering method was then incorporated in the model to ensure that the captured neurons are similar in brightness. As a result, the neural threshold may eventually converge to the cluster center of object, and leads a high performance of segmentation.

The rest of the paper is organized as follows. Section 2 briefly reviews the PCNN model and its principle of segmentation. Section 3 presents the proposed modified PCNN and the method for parameter setting. Section 4 demonstrates the high performance of the proposed model through infrared images. Finally, section 5 concludes our work and gives the prospects for further study.

2. PCNN Model

In this section, we briefly describe the original PCNN model and its principle of segmentation. The original PCNN model was developed by Eckhorn [1,18], which is a two-dimensional neural network. Each neuron in a network corresponds to a pixel in an input image, as shown in Figure 1. Generally, a pulse-coupled neuron consists of three main parts [19]: input field, modulation field, and pulse generator. The input field contains a feeding input F and linking input L. Each input communicates with neighboring neurons through the weights matrices M and W with the constant VF and VL, and retains their previous state through the exponential decay factors αF and αL, respectively. Particularly, the input F receives the external stimulus S, which corresponds to the intensity of a pixel in an input image I of size M * N. The significant characteristics of PCNN include the synchronous dynamic activity of neurons and periodic threshold dynamics. The inputs L and F are combined in the modulation field through the linking coefficient β to yield the internal activity U, which is compared to the previous state of the dynamic threshold E to produce the output Y in the pulse generator. If the neuron ij fires (Yij is set to 1), the threshold value VE will significantly increase. Thereafter, the corresponding threshold would decay through the time decay factor αE until the neuron fires again. The following equations describe the behavior of a single pulse-coupled neuron:

$$F_{ij}(n) = e^{-\alpha_F} F_{ij}(n-1) + V_F \sum_{k,l} M_{ij,kl} Y_{kl}(n-1) + S_{ij} \quad (1)$$

$$L_{ij}(n) = e^{-\alpha_L} L_{ij}(n-1) + V_L \sum_{k,l} W_{ij,kl} Y_{kl}(n-1) \quad (2)$$

$$U_{ij}(n) = F_{ij}(n)(1 + \beta L_{ij}(n)) \quad (3)$$

Figure 1. The Structure of Original PCNN Model.

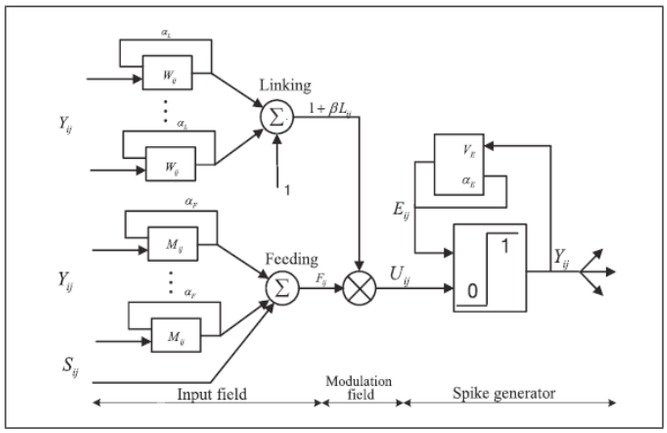

$$Y_{ij}(n) = \begin{cases} 1 & U_{ij}(n) > E_{ij}(n-1) \\ 0 & \text{others} \end{cases} \quad (4)$$

$$E_{ij}(n) = e^{-\alpha_E} E_{ij}(n-1) + V_E Y_{ij}(n) \quad (5)$$

where *kl* denotes the neighborhood of neuron *ij*. $M_{ij,kl}$ and $W_{ij,kl}$ represent the synaptic weights from the position of neuron *kl* to the position of neuron *ij*, respectively, and are expressed as follows:

$$M_{ij,kl}, W_{ij,kl} = \begin{cases} 0 & (i,j)=(k,l) \\ \frac{1}{\|(i,j)-(k,l)\|_2} & (i,j)\neq(k,l) \end{cases} \quad (6)$$

The neurons in the PCNN produce temporal series of pulse outputs through Eqs. (1)–(5) computation. This output contains information regarding the input image, which can be utilized for various image-processing applications such as image segmentation and feature generation. However, the determination of values for the PCNN parameters greatly increases the flexibility of this model in handling different images, and makes it hard to obtain the accuracy of the segmentation.

3. PCNN Modification and Parameter Adjustment

In this section, we present a modified model for image segmentation. In the proposed model, numerous parameters were reduced for simplification. The neuron threshold was also significantly changed compared to the original dynamic threshold. Furthermore, the proposed model does not require the setting of parameters through trial and error.

3.1. PCNN Modification

For years, several researchers have employed the original PCNN, which has numerous parameters that can be altered for behavior modification, to segment images and develop SPCNN-based image segmentation. However, the pulse behavior of a single neuron is affected by the dynamic threshold and the linking coefficient because of the biological background. In this paper, we present a novel neuron threshold, and develop an efficient algorithm for segmentation. Similar to the mathematical model of the PCNN, the proposed model is described by the following iterative process:

$$F_{ij}(n) = I_{ij} \quad (7)$$

$$L_{ij}(n) = \sum_{k,l} W_{ij,kl} Y_{kl}(n-1) \quad (8)$$

$$U_{ij}(n) = F_{ij}(n)(1 + \beta(n) \cdot L_{ij}(n)) \quad (9)$$

$$Y_{ij}(n) = \begin{cases} 1 & U_{ij}(n) > E_{ij}(n-1) \\ 0 & \text{others} \end{cases} \quad (10)$$

$$E_{ij}(n) = m_2(n) H_\varepsilon(m_2(n) - I_{ij}) \quad (11)$$

Where ahh notations have the same mening as indicated in Equs: (1)-(5) except for the regularized Heaviside function H_e which is as follows:

$$H_\varepsilon(z) = 1/2 \times (1 + 2/\pi \times \arctan(z/\varepsilon)) \quad (12)$$

Where ε affects the smoothness of the profile of the Heaviside function and is often used to control the transition of threshold from object to background .In Eq. (11), $m_2(n)$ represents the cluster center of the object under the specified condition that the pulse output Y of neurons divides the whole image in to the background(Y_{ij}=0) and object(Y_{ij}=1). Thus, $m_2(n)$ is obtained as follows:

$$m_2(n) = \sum_{i=1}^{M} \sum_{j=1}^{N} I_{ij} \times Y_{ij}(n) / \sum_{i=1}^{M} \sum_{j=1}^{N} Y_{ij}(n) \quad (13)$$

The cluster center of the background is then deduced as the following:

$$m_1(n) = \sum_{i=1}^{M} \sum_{j=1}^{N} I_{ij} \times (1 - Y_{ij}(n)) / \sum_{i=1}^{M} \sum_{j=1}^{N} (1 - Y_{ij}(n)) \quad (14)$$

To our knowledge, the overlap intensity of the background and object may occur in the interval [$m_1(n)$, $m_2(n)$] during PCNN iteration. Compared with existing PCNN models, the proposed model can adjust the behavior of neurons more easily. We removed the leaky integrator parts from the PCNN for the convenient adjustment of the internal activity. The threshold did not generate periodic oscillation and was shown as the combination of the cluster center and the Heaviside function. This is a key parameter setting.

The result implies that the neuron corresponding to its internal activity lower than m2(n) was prevented from firing. Besides, the parameters of the proposed model were reduced to the linking coefficient β to make the segmentation performance less sensitive to the parameter setting. When starting the segmentation task, a proper linking coeffcient value should be utilized to encourage the neurons with spatial proximity to fire. The captured neurons will then force the cluster center of the object to update, thus allowing for greater efficiency in controlling the pulse output. Through PCNN iteration, the cluster center may finally converge to the real cluster center and automatically achieve the final result. In the subsequent sections of the paper, we describe in detail the determination of a proper linking coefficient value.

3.2. Adjustment of Parameter β

In the proposed model, only the linking coefficient β should be adjusted. This parameter represents the linking strength of neurons and plays a significant role in neural behavior. This value is often determined by trial and error in previous studies. Generally, a large β value encourages low-brightness neurons to fire, whereas a small β value decreases the ability to capture neighboring neurons and maintains high similarity in the fired region. This may greatly increase the complexity in assigning a proper value to this parameter.

Therefore, we propose a method that can automatically determine the value of β. This method is inspired by Kuntimad et al.[10], who first analyzed the range of β to satisfy the conditions when the range intensity of adjacent regions overlap. For perfectimage segmentation, the value of β should be in the range $[\beta_{min},\beta_{max}]$, where:

$$\beta_{min} = max\{(I_4/I_3-1)/L_{Rmin}, (I_2/I_1-1)/L_{Bmin}\} \quad (15)$$

$$\beta_{max} = (I_4/I_2-1)/L_{Bmax} \quad (16)$$

In Eqs. (15) and (16), $[I_1, I_2]$ and $[I_3, I_4]$ are the intensity ranges of the background and the object, respectively, and often satisfy the inequality $I_1 < I_3 < I_2$. L_{Rmin} and L_{Bmin} denote the minimum linking input of the neural intensities I_3 and I_1 captured by the firing neurons, respectively. L_{Bmax} is the maximum linking input value of the neural intensity I_2 captured by the firing neurons (see [10] for details). To ensure that the neighboring neurons with similar brightness are captured, we determined the value of β during PCNN iteration

$$\beta(n) = (I_4(n)/I_2(n)-1)/L_{Bmax} \quad (17)$$

where the intensity $I_4(n)$ is the upper bound of the interval $[m_1(n), m_2(n)]$, and $I_2(n)$ is the average intensity of candidate-fired neurons, which receive the value of the linking input during PCNN iteration. The possible value of L_{Bmax} can be derived according to the linking radius r and the object–background boundary geometry. For the L-shaped region of the object, the value of L_{Bmax} for r=1.5 is equal ro $2+(0.5)^{0.5}$.

The varying value of β is significant in capturing neurons with spatial proximity. In contrast to the fixed value, the varying value of β allows the model to separate the intensity overlap more efficiently, considering that the intensity range $[m_1(n), m_2(n)]$ may be updated during PCNN iteration. Aside from coupling L_{Bmax}, the value of β was adjusted by the average intensity of the candidate-fired neurons. Thus, possible object neurons with spatial proximity were encouraged to fire, leading to a reasonable result.

3.3. Output Selection

The proposed method is an iterative algorithm, but may sensitive to the determination of linking coefficient value. Therefore, selecting the appropriate criterion is necessary to obtain the final result. According to extant literatures, the most straightforward method is to measure the regional similarity, such as minimum within-class variance [20], and/or entropy-based [2,13,21,22], before subsequently stopping the iteration. However, this method often requires all neurons to undergo the firing state, so that the results may be greatly affected by this criterion. To alleviate above problem and improve the segmentation performance, a possible solution is to incorporate a clustering method to avoid background neurons with spatial proximity from firing with a large value of β and ensure that neurons with similar brightness are captured. This is a significant procedure in our model. The clustering method is widely used in the field of pattern recognition [23]. In this paper, the Bayes clustering method was employed according to the principle of classification, which states that partitions the observations into the classes referring to the maximum a posterior probability. We firstly introduce the Bayes rule as follows:

$$p(x\in\Omega_c|I(x)) = \frac{p(I(x)|x\in\Omega_c)\cdot p(x\in\Omega_c)}{p(I(x))}, \quad c=1,2, \quad (18)$$

where x is the pixel position (i, j) of a simple representation in an input image I, $\Omega_1=\{x|\ Y_x(n)=0\}$, $\Omega_2=\{x|\ Y_x(n)=1\}$, $p(I(x)|x\in\Omega c)$ is the probability density in region Ω_c (c=1,2),and p(I(x)) is a prior probability of gray intensity I(x), which is independent of the chosen region and can be ignored.

Furthermore, $p(x\in\Omega c)$ can be ignored when the partition Ω_c (c=1,2) is assumed as priori equally possible, i.e., $p(x\in\Omega 1)= p(x\in\Omega 2)$.

The Bayesian classification forgiven $p(x\in\Omega c)$ and $p(I(x)|x\in\Omega c)$ is defined as follows:

$$\begin{aligned} &\text{if } p(x\in\Omega_2|I(x)) > p(x\in\Omega_1|I(x))\ Y_x = 1 \\ &\text{if } p(x\in\Omega_2|I(x)) \le p(x\in\Omega_1|I(x))\ Y_x = 0 \end{aligned} \quad (19)$$

where $Y_x=1$ and $Y_x = 0$ denote the neurons that belong to the object and background in position x, respectively. A decision can be made according to the value of

p(I(x)|x∈ Ωc). Therefore ,the firing state of candidate-fired neurons can be regulated as follows:

$$Y_x(n) = \begin{cases} 1 & p(I(x)|x\in\Omega_2) > p(I(x)|x\in\Omega_1) \\ 0 & p(I(x)|x\in\Omega_2) \leq p(I(x)|x\in\Omega_1) \end{cases}$$
$$\text{where } x \in \{x|L_x(n) > 0 \text{ and } Y_x(n-1) = 0\} \quad (20)$$

After classification, the pulse result Y(n) will be kept for next iteration. In Eq.(20), several approaches can be used to model the probability density p(I(x)|x∈Ωc), such as the Gaussian density [24] and non-parametric Parzen estimator [25]. In this paper, we assumed that the probability density p(I(x)|x∈Ωc) follows the Gaussian distribution:

$$p(I(x)|x\in\Omega_c) = \frac{1}{\sqrt{2\pi}\sigma_c}\exp\left(-\frac{(u_c - I(x))^2}{2\sigma_c^2}\right), \quad c = 1,2 \quad (21)$$

where u_c and σ_c are the intensity mean and standard deviation in region Ω_c (c = 1,2), respectively. Note that the role of the Bayes clustering method in the PCNN is rather subtle. This method has the potential for greater control over the behavior of neurons and the minimization of classification errors during iteration. In addition, it can avoid all neurons undergoing the firing state, thus allowing the model to potentially reduce the computational complexity. In summary, the neural threshold and linking coefficient are not completely independent of each other. The neural threshold could be seen as the result of the pulse output of neurons. The linking coefficient travels along the neural threshold for updates by incorporating the Bayes clustering method in the model.

4. Experiment and Comparison

In this section, we discuss the experimental results by using infrared images to demonstrate the efficiency of the proposed model. Generally, infrared imaging does not depend on the lighting condition but on temperature information. In many cases, the targets are warmer than the background, corresponding to the high brightness regions of the infrared image. However, a perfect extraction is often difficult to achieve because of several factors, such as inhomogeneous target brightness, low signal-to-noise ratio, blur boundary. Thus, segmenting infrared targets remain a challenge. Experiments were performed by using the MATLAB 7.10 on a computer with Intel(R) Core(TM) 2 Duo 2.4GHz i5 CPU 2G RAM, and windows 64 bit operation system. We initialized the linking coefficients as β = 0.30 and ε ¼ 1, and initialized the firing neurons that have the highest intensity in the image. Figure 2 shows the segmentation of several representative and challenging infrared images. Several targets exhibited small brightness regions in the image, which may result in unimodal histograms (Figure 2(a), (b), and (f)). Although warmer objects such as people tend to benoticeable in cooler backgrounds, the inhomogeneous brightness of these objects arises from their coverings (Figure 2(c)). In addition, intensity overlaps between the object and background often occurs (Figure 2(d) and (e)). Nevertheless, the proposed model is less sensitive to the above factors and can extract human targets with high accuracy from background (fourth row of Figure 2). To demonstrate the effectiveness of the proposed model, our strategy was compared with several kinds of segmentation algorithms, including Otsu's [26], k-means [27], Bazi's [24], and two similar versions of SPCNN (SPCNN1 and SPCNN2 by Ma [28] and Wei[2], respectively) with different parameter settings. Figure 3 shows the results of the above methods using the same infrared images. In Figure 3(a), Otsu's method failed to extract targets when the variance discrepancy between the targets and background was significant [29]. Furthermore, Otsu's method cannot segment images with intensity overlaps between the object and background. Figure 3(b) shows that the k-means method has mistaken several parts of the background as objects because the cluster centers were biased.

Particularly, a target segment was damaged in the bottom left (second row of Figure 3(b)), while the result of the proposed method was regarded as more acceptable. Bazi's method is a more general parametric approach that models the class distribution of a histogram as a general Gaussian distribution. However, the results obtained by Bazi's method were significantly affected by an unknown distribution of classes (Figure 3(c)). As can be seen, in all the test images, the segmentation results of proposed method were found to be better than the segmentation results obtained by these classic thresholding methods. Figure 3(d) and (e) shows the results of SPCNN1 and SPCNN2, respectively. In contrast to the threshold segmentation methods, the results generated by these two methods are somewhat sensitive to the parameter settings and the selection output criterion. It is clearly seen that the results are not desired. The CPU times of SPCNN1, SPCNN2, and the proposed model are provided in Table 1. As shown in this table, the proposed model.

Figure 2. **Application in real infrared image segmentation. Every column shows the original image, its histogram, the ground-truth targets manually delineated by red curves, and the segmentation results of proposed model. (For interpretation of the references to color in this figure caption, the reader is referred to the web version of this article.) (a) Image 1, (b) image 2, (c) image 3, (d) image 4, (e) image 5 and (f) image 6.**

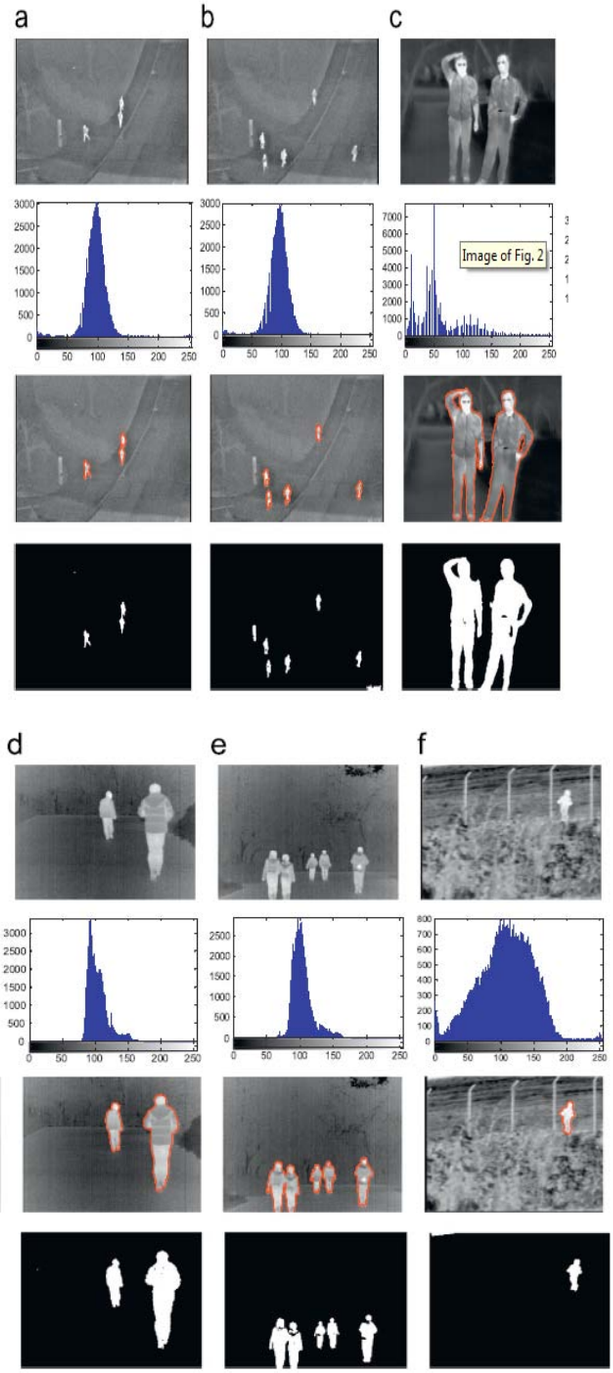

Figure 3. **Segmentation Results Obtained by Five Methods. (a) Otsu's, (b) k-means, (c) Bazi's, (d) SPCNN1 and (e) SPCNN2.**

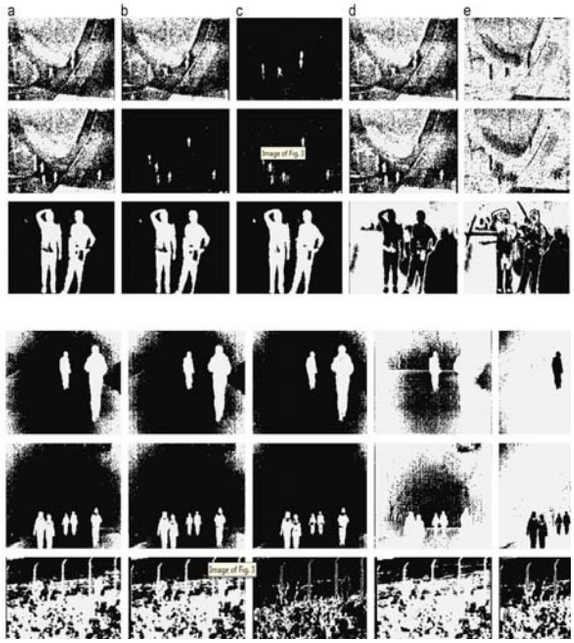

Table 1. **Computation Time of PCNN Model for Test Images (Second).**

Method	*Img.1*	*Img.2*	*Img.3*	*Img.4*	*Img.5*	*Img.6*
Spcnn1	0.4208	0.4079	0.3280	0.3354	0.3379	0.3237
Spcnn2	0.3862	0.3717	0.3308	0.3356	0.3535	0.3276
Proposed	0.1582	0.6816	1.3732	0.3322	0.3103	0.2723

utilized less CPU time when targets exhibited intensity homogeneity, such as in the results of Figure 2(a) and (f). For targets within homogeneous brightness, the proposed model utilized more time in increasing the segmentation performance. Figure4 shows the results of the original PCNN with a set of optimal parameter values. Such parameter values are usually determined by trial and error. In this work, we employed genetic algorithm to evolve the parameter values. In the genetic algorithm, the initial parameters are: the population size (S=50), crossover probability (Pc=0.9), mutation probability (PM=0.1), convergence threshold (δ=0.001), and fit function was established by minimizing the misclassification error (ME) [30]:

$$ME = 1 - \frac{|B_O \cap B_T| + |F_O \cap F_T|}{|B_O + F_O|} \quad (22)$$

Where BO and FO denote the background and foreground of the original image, respectively; BT and FT denote

the separated back ground and foreground, respectively; denotes the cardinality of the set. Table 2 presents the evolved parameter values for the test images. Such parameter values enable the PCNN to obtain good results through the heavy evolving process. However, we notice that the results are often affected by the blur boundary of human targets, as shown in the first and second image in Figure4. Additionally, the model is somewhat sensitive to the noise, as seen the fourth and fifth image in Figure4. By modifying the original PCNN, our model can cope with these problems, and avoid the repetition of trails and a heavy training. This demonstrates the advantage of the proposed model in terms of segmentation accuracy and ease of use. For the assessment of the performances of the above segmentation methods, several performance measurement schemes for image segmentation were used, such as edge mismatch [30].

Figure 4. The Segmentation Results of PCNN with Optimal Parameter Values Evolved by GA Method.

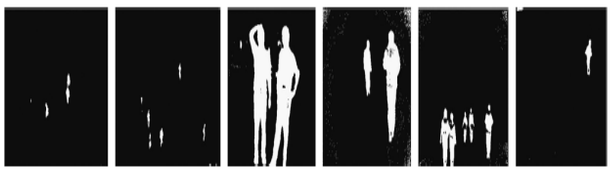

Table 2. Optimal Parameter Values Evolved by Genetic Algorithm for Test Images.

Test Image	α_L	V_L	β	α_F	V_F	α_E	V_E	n	W/M
Img.1	0.9922	1.0	0.8677	0.9027	1.0	0.0506	118.0739	33	$\begin{bmatrix} 1/2 & 1 & 1/2 \\ 1 & 0 & 1 \\ 1/2 & 1 & 1/2 \end{bmatrix}$
Img.2	0.3035		0.2685	0.7354		0.0895	250.0389	14	
Img.3	0.1323		0.2490	0.7588		0.0156	150.8171	11	
Img.4	0.7977		0.5564	0.9572		0.0078	249.0467	7	
Img.5	0.5136		0.2296	0.9144		0.0156	127.9961	9	
Img.6	0.0778		0.1595	0.6148		0.0039	231.1868	22	

Table 3. ME of Test Images Obtained by Different Methods.

Method	*Img.1*	*Img.2*	*Img.3*	*Img.4*	*Img.5*	*Img.6*
Otsu's	0.5294	0.5022	0.0271	0.1896	0.1092	0.5402
k-means	0.5181	0.0041	0.0271	0.1423	0.0813	0.5305
Bazi's	0.0245	0.0276	0.0184	0.0465	0.0237	0.2621
Spcnn1	0.5632	0.5351	0.7447	0.5997	0.6526	0.6375
Spcnn2	0.7946	0.7687	0.6546	0.9429	0.9462	0.3872
Pcnn	0.0023	0.0048	0.0190	0.0182	0.0203	0.0032
Proposed	0.0003	0.0053	0.0146	0.0013	0.0048	0.0021

region contrast [31], and ME. For infrared target extraction, we employed the ME to evaluate the segmentation performance (Eq. (22). Ground-truth targets were manually delineated by red curves (third row of Figure 2). Table 3 lists the misclassification error obtained by using segmentation methods, where ME varies from 0 for desired segmentation to 1 for failure of segmentation. The results show that the proposed method has fewer ME than the other segmentation methods, thus verifying the high performance of the proposed method.

5. Conclusion and Future Work

An efficient iterative algorithm was presented in this paper for automatic image segmentation using a modified PCNN. We disregarded the mechanism of the dynamic threshold and presented a new adaptive neural threshold that can efficiently control the pulse output of neurons. By incorporating the Bayes clustering method, the varying linking coefficient value enables the model to segment a wide range of images efficiently and achieve satisfactory results for targets with inhomogeneous brightness. Experiments on real-world infrared images demonstrate the high performance of the proposed method. In near future work, two aspects can improve segmentation performance. First, the linking coefficient can be localized to encourage neighboring neurons with similar local regions to pulse together. Second, other types of probability densities $p(I(x)|x \in \Omega c)$ should be considered because the distribution of the background or object may not obey the Gaussian distribution.

References

[1] Eckhorn, R., Reitboeck, H. J., Arndt, M. & Dicke, P. (1990). Feature linking via synchronization among distributed assemblies: Simulations of results from cat visual cortex. *Neural Computing*, 2, 293-307.

[2] Wei, S., Hong, Q. & Hou, M. (2011). Automatic image segmentation based on PCNN with adaptive threshold time constant. *Neuro Computing*, 74(9), 1485-1491.

[3] Chen, X. & Chai, X. (2010). Infrared image segmentation based on a simplified PCNN. *Journal of Anhui University, Natural Science Education*, 34(1), 74-77.

[4] Waldemark, K., Lindblad, T., Bečanović, V., Guillen, J. L. L. & Klingner, P. L. (2000). Patterns from the sky: Satellite image analysis using pulse coupled neural networks for pre-processing, segmentation and edge detection. *Pattern Recognition Letters*, 21(3), 227-237.

[5] Na, Y., Chen, H., Li, Y. & Hao, X. (2012). Coupled parameter optimization of PCNN model and vehicle image segmentation. *Journal of Transportation Systems Engineering and Information Technology*, 12(1), 48-54.

[6] Peng, Z., Jiang, B., Xiao, J. & Meng, F. (2008). Novel method of image segmentation based on parallelized firing PCNN. *Acta Automatica Sinica*, 34(9), 1169-1173.

[7] Kong, X., Huang, J. & Shi, H. (2001). *Improved pulse coupled neural networks for target segmentation in infrared images*. Proceedings of SPIE, 4555, 81-86.

[8] Karvonen, J. A. (2004). *Baltic sea ice SAR segmentation and classification using modified pulse-coupled neural networks*. IEEE Transactions of Geoscience and Remote Sensing, 42(7), 1566-1574.

[9] Wang, Z., Ma, Y., Cheng, F. & Yang, L. (2010). Review of pulse coupled neural networks. *Image Vision Computing*, 28(1), 5-13.

[10] G. Kuntimad, H.S. Ranganath, (1999). *Perfect image segmentation using pulse coupled neural networks*, IEEE Transaction Neural Networks, 10(3), 591-598.

[11] Kinser, J. M. (1996). *A simplified pulse-coupled neural network*. Proceedings of SPIE, 2760, 563-569.

[12] Chen, Y., Park, S., Ma, Y. & Ala, R. (2011). *A new automatic parameters setting method of a simplified PCNN for image segmentation*. IEEE Transactions of Neural Networks, 22(6), 880-892.

[13] Ma, Y., Zhan, K. & Qi, C. (2008). Study on self-adaptive pulse coupled neural network and its application in fields of image processing. *Journal of System Stimulation*, 20(11), 2890-2897.

[14] Ma, Y. & Qi, C. (2006). Study of automated PCNN system based on genetic algorithm. *Journal of System Stimulation*, 18(3), 722-725.

[15] Bi, Y., Qiu, T., Li, X. & Guo, Y. (2004). Automatic image segmentation based on a simplified pulse coupled neural network. *Lecture Notes in Computer Science*, 3174, 405-410.

[16] Rava, T. H., Bettaiah, V. & Ranganath, H. S. (2011). Adaptive pulse coupled neural network parameters for image segmentation. *World Academy of Science, Engineering and Technology*, 73, 1046-1054.

[17] Deng, X. & Ma, Y. (2012). PCNN model automatic parameters determination and its modified model. *Acta Electronica Sinica*, 40(5), 955-965.

[18] Echnorn, R., Bauer, R., Jordan, W. & Brosch, M. (1988). Coherent oscillations: A mechanism of feature linking in the visual cortex? *Biological Cybernetics*, 60, 121-130.

[19] Lindblad, T. & Kinser, J. M. (2005). *Image Processing using Pulse-Coupled Neural Networks* (2nd ed.) Germany, Berlin: Springer.

[20] Wang, H., Zhang, K. & Li, Y. (2005). Image segmentation method based on PCNN. *Opto-Electronic Engineering*, 32(5), 93-96.

[21] Liu, Q., Ma, Y. & Qian, Z. (2005). Automated image segmentation using improved PCNN model based on cross-entropy. *Journal of Image and Graphics*, 10(5), 579-584.

[22] Ma, Y., Dai, R. & Li, L. (2002). Automated image segmentation using pulse coupled neural networks and image's entropy. *Journal of China Institute of Communications*, 23(1), 46-51.

[23] Duda, R. O., Hart, P. E. & Stork, D. G. (2001). *Pattern Classification* (2nd ed.).Wiley.

[24] Bazi, Y., Bruzzone, L. & Melgani, F. (2007). Image thresholding based on the EM algorithm and the generalized Gaussion distribution. *Pattern Recognition*, 40(2), 619-634.

[25] Kim, J., Fisher, J., Yezzi, A., Cetin, M. & Willsky, A. (2002). *Non-parametric methods for image segmentation using information theory and curve evolution*. IEEE International Conference on Image Processing, 3, 797-800.

[26] Otsu, N. (1979). *A threshold selection method from gray-level histogram*. IEEE Transactions on Systems, Man and Cybernetics, 9(1), 62-66.

[27] Kanungo, T. & Mount, D. M. (2002). *An efficient k-means clustering algorithm: Analysis and implementation*. IEEE Transactions on Pattern Analysis and Machine Intelligence, 24 (7), 881-892.

[28] Ma, Y., Dai, R. & Li, L. (2002). Image segmentation of embryonic plant cell using pulse-coupled neural networks. *Chinese Science Bulletin*, 47(2), 167-172.

[29] Xu, X., Xu, S., Jin, L. & Song, E. (2011). Characteristic analysis of Otsu threshold and its applications. *Pattern Recognition Letters*, 32(7), 956-961.

[30] Sezgin, M. & Sankur, B. (2004). Survey over image thresholding techniques and quantitative performance evaluation. *Journal of Electronic Imaging*, 13(1), 146-168.

[31] Levine, M. D. & Nazif, A. M. (1985). *Dynamic measurement of computer generated segmentation*. IEEE Transactions on Pattern Analysis and Machine Intelligence, 7(2), 155-164.